

# Variable wavelength interferometry

## VIII. Calibration

MAKSYMILIAN PLUTA

Central Optical Laboratory, ul. Kamionkowska 18, 03-805 Warszawa, Poland.

Determination of the relationship between the light wavelength and the interfringe spacing is a basic calibration operation in interferometry. A simple and accurate method of the calibration of double refracting microinterferometers is proposed. The method is based on the object-adapted variable wavelength interferometry (AVAWI) developed recently and described in the preceding paper of this series. Only a birefringent plate of known thickness or a glass plate with a narrow groove (or a step) of known depth are required for the calibration process. Its important advantage lies in the fact that it can be performed under the conditions of the normal use of the microinterferometer.

### 1. Introduction

For VAWI techniques discussed formerly, the relationship between the interfringe spacing  $b$  and the light wavelength  $\lambda$  must be known very accurately within the visible spectrum. If highly monochromatic (e.g., laser) light is used, the interfringe spacing  $b$  is one of the most precisely determined parameters in interferometry. If, however, the light used is moderately monochromatic, say, it is selected from a white light source by means of conventional interference filters, there are some problems with the accurate determination of the ratio  $\lambda/b$  for visual interferometry in the long-wavelength (red) and short-wavelength (blue) regions of the visible spectrum. From [1] and [2] it follows that an interferometer which has been calibrated in highly monochromatic light cannot be qualified, in general, as a high precision instrument when a source of highly monochromatic light used for the calibration will then be replaced by a source of moderately monochromatic light.

To overcome the above limitation, a new calibration procedure is proposed; it uses that light source which is offered to the user as a standard equipment of his microinterferometer. The procedure depends on the use of the object-adapted variable wavelength interferometry (AVAWI) developed recently and described in [3] (alternatively, quasi-adaptive (QA) version of the VAWI-1 technique can also be used). Only a birefringent plate of known thickness  $t$  (Fig. 1a) or a glass plate with a narrow groove of depth  $d$  (Fig. 1b) is required for the calibration process.

As previously [3], a double-refracting microinterferometer, the Biolar PI, is taken into consideration. Its optical system is shown in Fig. 2. Its birefringent prisms  $W_0$ ,  $W_1$  and  $W_2$  are made of quartz crystal. Consequently, the calibration birefringent plate (Fig. 1a) is also made of quartz crystal. The plate is cut parallel to the optic

(crystalline) axis and is primarily used for the calibration of the transmitted-light interference system (shown in Fig. 2), while the glass plate with a narrow groove (Fig. 1b) is recommended for the calibration of this system equipped with an epi-illuminator for reflected-light microinterferometry. The reflected-light calibration can also be performed with the help of a step glass plate (Fig. 1c) which is easier for manufacturing than the groove plate (Fig. 1b).

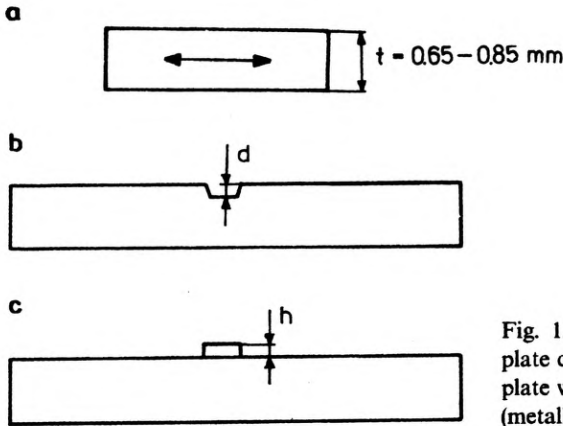


Fig. 1. Calibration objects: **a** – birefringent (quartz) plate cut parallel to the optic axis of crystal, **b** – glass plate with a narrow groove, **c** – glass plate with a step (metallized)

The thickness  $t$  of the quartz plate (Fig. 1a), the depth  $d$  of the groove (Fig. 1b), and the height  $h$  of the step (Fig. 1c), must be known extremely precisely, say,  $\Delta t/t = \Delta d/d = \Delta h/h = 0.01\%$  or at least  $0.05\%$ . It is self-evident that such a small inaccuracy in determining  $t$ ,  $d$  or  $h$  can be obtained using a high precision instrument, especially an interferometer or a low-power microinterferometer fitted with a highly monochromatic light source, say, He-Ne laser. In particular, the Biolar PI microinterferometer may be used for this measurement if it has primarily been calibrated in highly monochromatic light and then the same light is used for determining  $t$ ,  $d$  or  $h$ . Moreover, it is also self-evident that these parameters should be given by the manufacturer of the calibration plates. For example, the Zeiss (Jena) microrefractometric plates (see [4] and [5]) can be qualified as the calibrating plates of the groove type (Fig. 1b). The depth  $d$  of their groove is given by the manufacturer with an inaccuracy  $\Delta d = 0.0005 d$ .

## 2. Calibration in transmitted light

The calibration in transmitted light can be performed using either the quartz plate (Fig. 1a) and the adaptive VAWI-3 technique or the groove plate (Fig. 1b) and the VAWI-1 technique. The first technique functions in the interfringe spacing domain and is denoted by AVAWI(b)-3, while the other pertains to the original VAWI method [4].

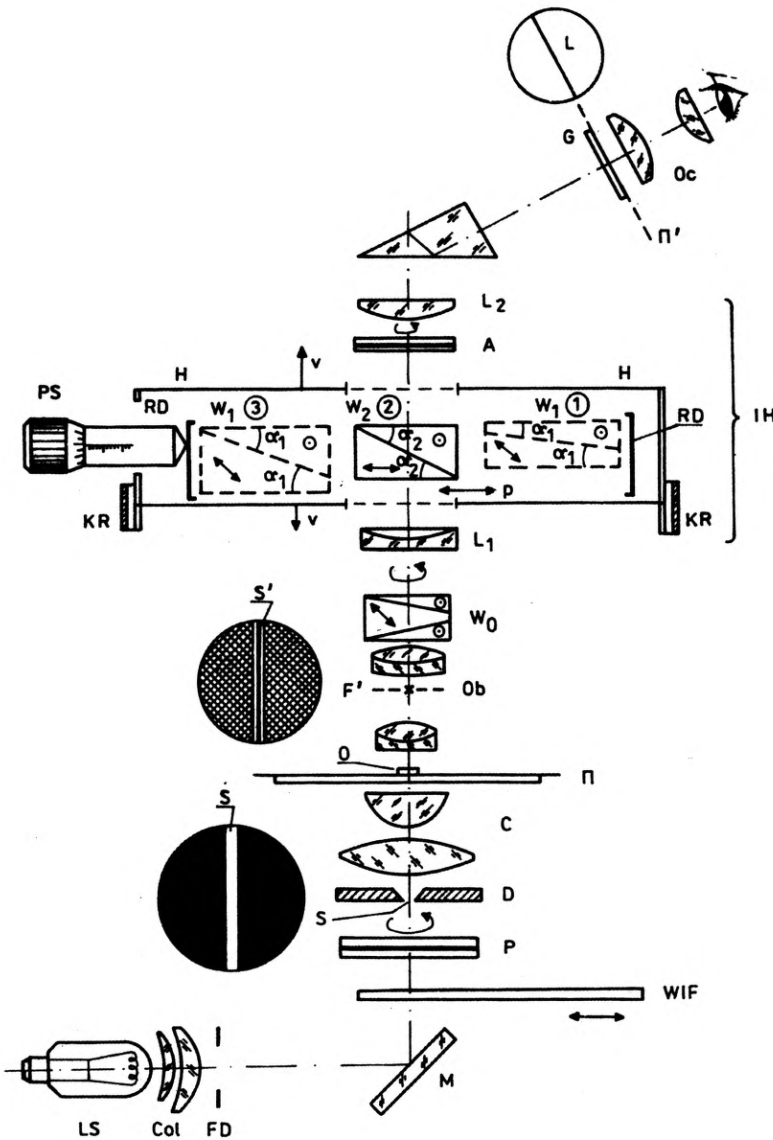


Fig. 2. Optical system of the double refracting microinterferometer Biolar PI. LS – light source (halogen lamp 12 V/100 W), Col – collector, FD – field diaphragm, M – mirror, WIF – wedge interference filter (Veril S 200, Schott Glaswerke, Mainz), P – polarizer, D – slit diaphragm, S – slit coincident with the front focal point of the condenser C,  $\Pi$  – object plane, O – calibration object (see Fig. 1), Ob – objective (that of magnifying power  $10\times$  was used for the calibration in question),  $F'$  – back focal plane of the objective,  $S'$  – image of the slit S (this image is coincident with  $F'$ ),  $W_0$  – objective birefringent prism (this prism can be rotated round the objective axis),  $L_1$  and  $L_2$  – tube lenses,  $W_1$  and  $W_2$  – tube birefringent prisms installed in a revolving disc RD, KR – knurled ring for adjusting the prisms  $W_1$  and  $W_2$  along the vertical ( $v$ ) direction, PS – micrometer (phase) screw for moving the birefringent prisms  $W_1$  and  $W_2$  along the transverse direction marked by the arrowed line p, H – holder of the revolving disc RD with the birefringent prisms, A – analyser, IH – interferometric head,  $\Pi'$  – image plane coincident with the front focal plane of a microscope ocular Oc, G – ocular focal plate with a pointer line L.

### 2.1. The AVAWI(*b*)–3 technique

The calibration procedure is based on the following equations [3]:

$$\frac{\lambda_s}{B_s} = \frac{t}{m_1 + q_s} = \frac{t}{m_s} \quad (1)$$

where

$$m_1 = q_s \frac{b_s}{b_1 - b_s}, \quad (2)$$

and

$$\bar{b}_s = \frac{\bar{C}}{m_s} = \frac{C_L + C_R}{2m_s}, \quad (3)$$

where  $C = (C_L + C_R)/2$ , and  $C_L$  and  $C_R$  are defined as

$$C = \overline{m_s b_s} = \frac{\sum_{s=1}^S m_s b_s}{S}. \quad (4)$$

Here the subscript *s* is equal to 1, 2, 3, ... and denotes the successive situations (*s*) when the interfringe spacings  $b_s = b_1, b_2, b_3, \dots$  are measured by means of the micrometer (phase) screw PS linked to the transverse movement (*p*) of the tube birefringent prisms  $W_1$  and  $W_2$  (Fig. 2);  $B_s = B_1, B_2, B_3, \dots$  are the birefringences (for  $\lambda_s = \lambda_1, \lambda_2, \lambda_3, \dots$ ) of crystalline quartz of which the prisms  $W_1, W_2$  and calibration plate QP are made;  $m_1$  is an integer number referred to as the initial interference order at the pointer line *L*;  $m_s$  is the current interference order and  $q_s$  is the increment of this order which respect to  $m_1$ , i.e.,  $m_s = m_1 + q_s$ , when the light wavelength is decreased from  $\lambda_s = \lambda_1$  to  $\lambda_s = \lambda_2, \lambda_3, \lambda_4, \dots$  (the increments  $q_s$  are sequentially observed at the pointer line *L*), and *t* is the thickness of the calibration quartz plate (QP). The subscripts L and R refer to the left-handed and right-handed diagonal positions (Figs. 3b and c) of the plate QP. In these positions the plate QP, due to its birefringence, displaces maximally in opposite directions the interference fringes of the microinterferometer in question. The left-handed and right-handed diagonal positions are achieved by rotating the calibration plate through  $+45^\circ$  and  $-45^\circ$  starting from its neutral position (Fig. 3a) for which the interference fringes remain in their original position determined by the empty interference field (i.e., without the calibration plate). The quantities  $C_L$  and  $C_R$  are the mean products  $\overline{m_s b_s}$  which follow from formula (4), where *S* is the overall number of coincidences of the interference fringes of consecutive current orders  $m_s$  with the pointer line *L* (Fig. 2) or the image *S'* of the condenser slit *S*, when the light wavelength is decreased from  $\lambda_s = \lambda_1$  to  $\lambda_s = \lambda_2, \lambda_3, \lambda_4, \dots$  by means of the wedge interference filter WIF (Veril S 200, Schott Glaswerke, Mainz). The coincidences of interference fringes with the pointer line *L* apply to the birefringent prism  $W_2$  No. 2, which produces fringe-field interference in the image plane  $\Pi'$  of the microinterferometer, while the coincidences of fringes

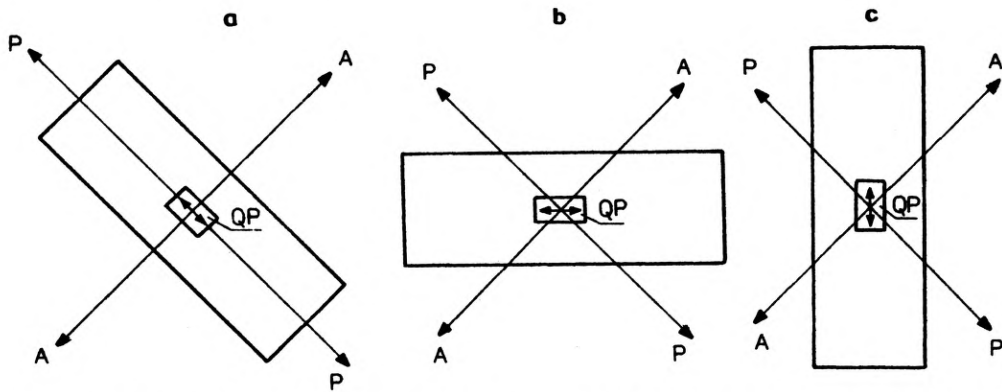


Fig. 3. Neutral (a), left-handed (b) and right-handed (c) positions of the calibration birefringent plate shown in Fig. 1a. PP and AA – transmission axes of the polarizer P (Fig. 2) and the analyser A. The optic (crystalline) axis of the calibration plate is marked by the arrowed line. This plate is mounted, for convenience, in a metallic frame

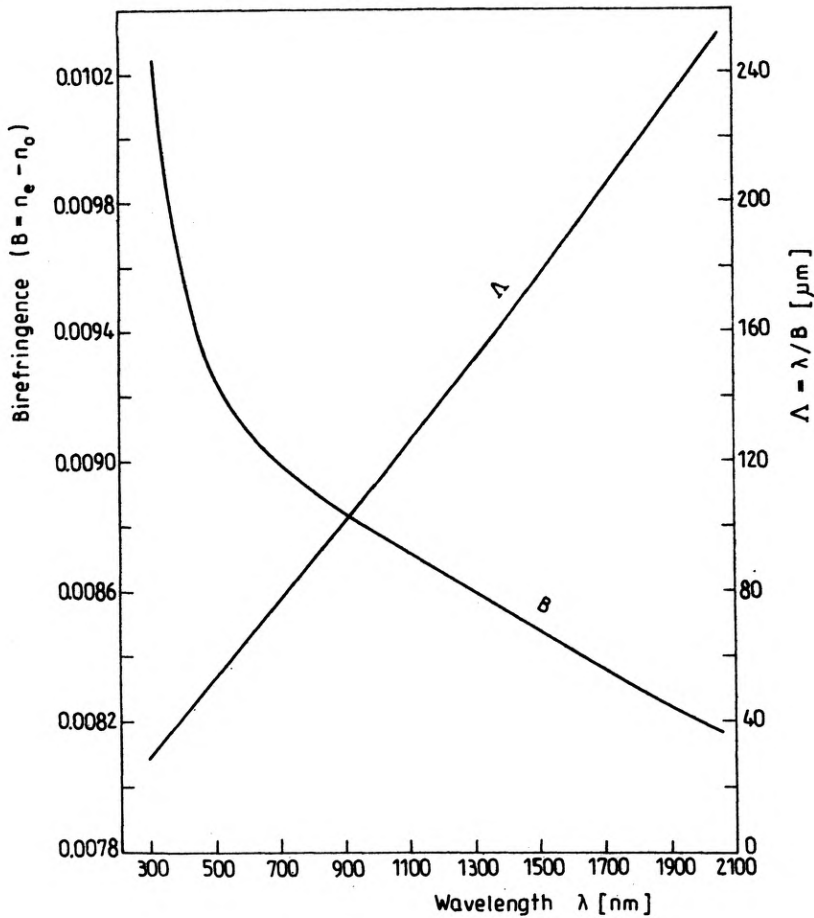


Fig. 4. Plots of the quartz birefringence  $B$  and of the ratio  $A = \lambda/B$  as a function of the light wavelength  $\lambda$

with the slit image  $S'$  refer to the prisms  $W_1$  No. 1 and  $W_1$  No. 3, which produce uniform-field interference in the image plane  $\Pi'$ . To observe the image  $S'$  the microscope ocular (Oc) with the pointer line  $L$  is replaced by an auxiliary low-power microscope with long working distance.

The calibration process is as follows. Starting from its red end, the interference filter WIF is transversely slit to select from white light such particular wavelengths  $\lambda_s = \lambda_1, \lambda_2 < \lambda_1, \lambda_3 < \lambda_2, \dots$  for which the consecutive coincidences of the centres of interference fringes with the pointer line  $L$  or slit image  $S'$  are observed, together with the sequential increments  $q_s$ . Each coincidence achieved is followed by the measurement of the interfringe spacing  $b_s$  associated with the respective light wavelength  $\lambda_s$ . The measurement of multiple interfringe spacings, e.g., the distance  $d = 40b_s$  between interference fringes of plus and minus twenty orders (when the prism  $W_2$  is calibrated), rather than a single interfringe spacing is recommended leading to more accurate values for  $b_s$ . This measurement is of course performed by means of the phase screw PS, whose scale can be read out with an accuracy  $\pm 1 \mu\text{m}$ . It is also recommended to select  $q_s = 0, 1, 2, 3, \dots$ , respectively, for  $m_s = m_1, m_1 + 1, m_1 + 2, m_1 + 3, \dots$ . In such a situation the centres of black fringes coincide with the pointer line  $L$  or the slit image  $S'$ . However,  $q_s = 0.5, 1.5, 2.5, \dots$  can also be used. These increments produce  $m_s = m_1 + 0.5, m_1 + 1.5, m_1 + 2.5, \dots$  and are observed when the centres of bright interference fringes are brought into consecutive coincidences with the pointer line  $L$  or the slit image  $S'$ .

The ratios  $A = \lambda_s/B_s$  are then calculated from Eq. (1) and the wavelengths  $\lambda_s$  are read out from graph  $A(\lambda)$  shown in Fig. 4. The wavelengths  $\lambda_s$  can be also calculated from the following equation:

$$\lambda_s = \lambda + \frac{A_s - A}{T} \quad (5)$$

where  $A = \lambda/B$  and  $T = \Delta A/\Delta \lambda$  are given in Table 1 (in fact,  $T$  is the local tangent of the plot  $A(\lambda)$  shown in Fig. 4).

Finally, the calibration plot  $b(\lambda)$  is made of a series of  $\lambda_s$  and respective  $b_s$ .

For a complete clarity, the entire calibration process is summarized in Table 2. No further comments are necessary except the initial interference order  $m_1$ . This integer number can be calculated from Eq. (2), but due to the fact that the conditions of the AVAWI( $b$ ) method are fulfilled, we can simply observe the maximum displacement of the zero-order interference fringe and count the number of the interfringe spacings  $b_1$  between the displaced and undisplaced zero-order fringes when the wedge interference filter is adjusted to the wavelength  $\lambda_1$ . These fringes are ready recognizable in white light since they are achromatic (dark).

## 2.2. The VAWI-1 technique

This technique uses a groove calibration plate (Fig. 1b) and the following equation:

$$\frac{\lambda_s}{n_s - 1} = \frac{d}{m_1 + q_s} = \frac{d}{m_s} \quad (6)$$

Table 1. Ratios  $A$  of the light wavelengths  $\lambda$  to the respective birefringences  $B$  of natural quartz crystals, and local tangents  $T = \Delta A / \Delta \lambda$  of the plot  $A(\lambda)$  shown in Fig. 4 (birefringences  $B$  taken from Ref. [3] and Ref. [7] cited in [3])

$\lambda$ [nm]	$A = \lambda/B$ [nm]	$T$	$\lambda$ [nm]	$A = \lambda/B$ [nm]	$T$	
300	29182.9	127.6	625	68954.1	118.9	
325	32383.1		643.847 (C)	71269.3		
350	35565.5		650	71934.5		
375	38663.8	124.5	656.278 (C)	72677.5		
400	41779.8		675	74900.1		
425	44873.8		700	77881.6		
450	47913.1	121.4	725	80825.0		120.1
475	50949.3		750	83817.6		
479.991 (F')	51556.5		775	86815.3		
486.133 (F)	52294.9		800	89796.8		
500	53984.0	120.3	825	92811.3		
525	56978.5		850	95807.0		
546.072 (e)	59510.9		875	98814.2		
550	59978.2		900	101844.5		
575	62979.2		925	104851.5		
587.563 (d)	64482.3		950	107856.5		
589.290 (D)	64693.2		975	110845.8		
600	65970.3		1000	113895.2		

Table 2. Algorithm of the calibration of the double refracting microinterferometer Biolar PI by using a birefringent (quartz) plate of known thickness  $t$  and the AVAWI(b)-3 technique

$s$	$q_s$	$\frac{b_s}{L \quad R}$		$m_s$	$\frac{m_s b_s}{L \quad R}$		$\bar{b}_s = \frac{\bar{C}}{m_s}$	$A_s = \frac{\lambda_s}{B_s} = \frac{t}{m_s}$	$\lambda_s$
1	$q_1 = 0$	$b_1$	$b_1$	$m_1$	$m_1 b_1$	$m_1 b_1$	$\bar{b}_1$	$A_1$	$\lambda_1$
2	$q_2$	$b_2$	$b_2$	$m_2 = m_1 + q_2$	$m_2 b_2$	$m_2 b_2$	$\bar{b}_2$	$A_2$	$\lambda_2$
3	$q_3$	$b_3$	$b_3$	$m_3 = m_1 + q_3$	$m_3 b_3$	$m_3 b_3$	$\bar{b}_3$	$A_3$	$\lambda_3$
...	...	...	...	...	...	...	...	...	...
S	$q_S$	$b_S$	$b_S$	$m_S = m_1 + q_S$	$m_S b_S$	$m_S b_S$	$\bar{b}_S$	$A_S$	$\lambda_S$

$$C_L = \overline{m_s b_s} = \frac{1}{S} \sum_{s=1}^S m_s b_s; \quad C_R = \overline{m_s b_s} = \frac{1}{S} \sum_{s=1}^S m_s b_s; \quad \bar{C} = \frac{C_L + C_R}{2}$$

where

$$m_1 = q_s \frac{\lambda_s}{N_{s1} \lambda_1 - \lambda_s}, \tag{7}$$

and

$$N_{s1} = \frac{n_s - 1}{n_1 - 1}. \quad (8)$$

Here  $d$  is the groove depth,  $n_s = n_1, n_2, n_3, \dots$  are the refractive indices (for the light wavelengths  $\lambda_s = \lambda_1, \lambda_2, \lambda_3, \dots$ ) of an optical glass of which the calibration plate is made, while  $q_s, m_s$  and  $m_1$  are the same parameters as in Eq. (1). The subscript  $s$  runs through 1, 2, 3, ...

The calibration process is now as follows. The calibration plate is oriented so that its groove forms an angle of  $90^\circ$  in the object plane  $\Pi$  (Fig. 2) with the interference fringes observed in the image plane  $\Pi'$  while the objective birefringent prism  $W_0$  is crossed with the tube birefringent prism  $W_2$  No. 2 (the tube prisms  $W_1$  No. 1 and  $W_1$  No. 2 are ignored for the moment). Under these conditions two sheared images of the groove are observed with interference fringes  $I'$  displaced in the opposite directions relative to the fringes  $I$  of the empty interference field, i.e., not perturbed by the groove (Fig. 5). Sliding the wedge interference filter (WIF, Fig. 2) permits us to

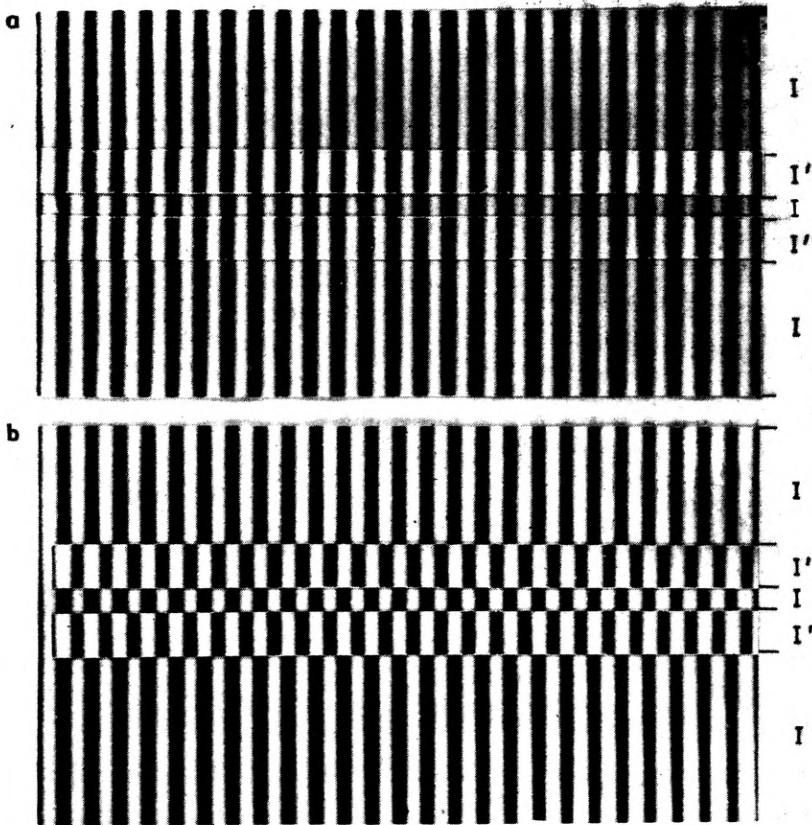


Fig. 5. Coincident (a) and anticoincident (b) configurations of the reference (undisplaced) interference fringes  $I$  and the fringes  $I'$  displaced in the totally sheared images of a narrow groove of the calibration plate shown in Fig. 1b



select such an initial wavelength  $\lambda_1$  in the red spectral region, for which the interference fringes  $I$  and  $I'$  become coincident with each other. This situation is just shown in Fig. 5a. The interfringe spacing  $b_1$  is then measured by means of the phase screw PS (Fig. 2). This spacing and  $\lambda_1$  are related with a current interference order  $m_s = m_1$  for which  $q_s = 0$ . Further decreasing  $\lambda$  by sliding the wedge interference filter leads to the second particular wavelength  $\lambda_2$  for which the fringes  $I'$  become anticoncident with the fringes  $I$  as shown in Fig. 5b. We have now  $q_s = 0.5$ ,  $m_s = m_1 + 0.5$ , and  $b_s = b_2$ . This latter parameter is measured, and next the above operations are repeated to select the further particular wavelengths  $\lambda_3, \lambda_4, \lambda_5, \dots$ , for which the consecutive coincident and anticoncident configurations of the fringes  $I'$  and  $I$  appear. These configurations give the interfringe spacings  $b_s = b_3, b_4, b_5, \dots$  which are measured, the increments  $q_s = 1, 1.5, 2, \dots$  are observed, thus  $m_s = m_1 + 1, m_1 + 1.5, m_1 + 2, \dots$  are fixed. The ratios  $A_s = \lambda_s / (n_s - 1)$  are then calculated from Eq. (6) and  $\lambda_s$  are read out from the plot  $A(\lambda)$ , and the initial interference order  $m_s$  is

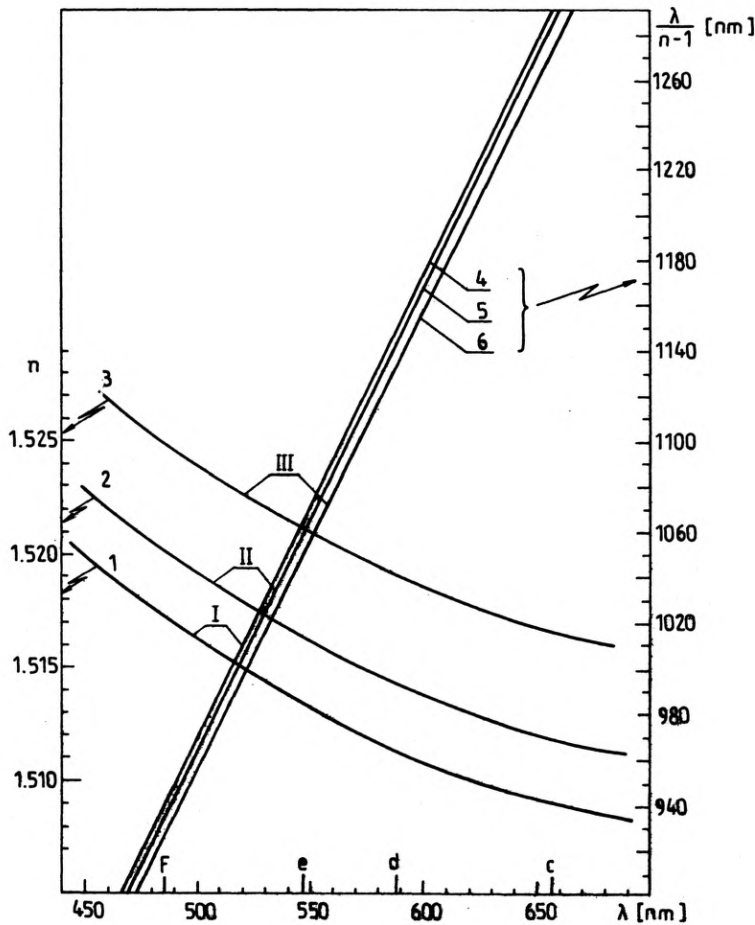


Fig. 6. Plots of the spectral dispersion of refractive index and of the ratios  $A = \lambda / (n - 1)$  for the Zeiss microrefractometric plates whose parameters are listed in Table 3

calculated from Eq. (7). Finally, the calibration plot  $b(\lambda)$  can be made of a series of  $\lambda_s$  and  $b_s$ .

Figure 6 shows three slightly different graphs (4, 5 and 6) of the ratio  $A = \lambda/(n-1)$  as a function  $\lambda$  for three calibration plates made of an optical glass whose spectral dispersions of the refractive index  $n$  differ from each other (curves 1, 2 and 3). In fact, this figure illustrates the optical properties of a set of microrefractometric plates manufactured by VEB Carl Zeiss (Jena) as the standard equipment of the Interphako microscopes. These plates have a narrow groove and are qualified (by the author of this paper) as good objects for the calibration in question. Their basic refractive indices and the depth ( $d$ ) of groove are given in Table 3.

Table 3. Basic refractive indices  $n_F$ ,  $n_e$ ,  $n_d$ , and  $n_C$ , ratios  $A_i = \lambda_i/(n_i-1)$ , where  $i = F, e, d, \text{ and } C$ , and the groove depths  $d$  of a standard set of three refractometric plates available commercially from C. Zeiss Jena

Plate (Factory number)	Wavelength [nm]	$n$	$A$ [nm]	$d$ [ $\mu\text{m}$ ]
I (620575)	486.1 (F)	1.51703	940.17755	10.0230
	546.1 (e)	1.51333	1063.83808	
	587.6 (d)	1.51133	1149.16003	
	656.3 (C)	1.50893	1285.56831	
II (620561)	486.1	1.51989	935.00548	12.5425
	546.1	1.51619	1057.94378	
	587.6	1.51419	1142.76824	
	656.3	1.51179	1282.36191	
III (620566)	486.1	1.52470	926.43415	13.3762
	546.1	1.52100	1048.17658	
	587.6	1.51900	1132.17726	
	656.3	1.51660	1270.42199	
$\Delta n = 0.0002$				$\Delta d = 0.0005d$

The same plates can also be used for the calibration of the birefringent prisms  $W_1$  No. 1 and  $W_1$  No. 3 (Fig. 2). However, these prisms produce the uniform-field interference pattern in the image plane  $\Pi'$ , and the coincident and anticoincident configurations of interference fringes  $I'$  and  $I$  are no longer achieved (Fig. 5). The principles of the uniform-field VAWI method must, therefore, be employed (see [6], for details).

### 3. Calibration in reflected light

The calibration  $b(\lambda)$  in reflected light refers to the Biolar PI microscope equipped with an epi-illuminator (see Figs. 3 and 4 in [5]).

In epi-illumination the relation between the interfringe spacing  $b$  and the light wavelength  $\lambda$  has the same character as that for dia-illumination discussed until now,

but the interfringe spacings  $b_s$  (in general  $b$ ) are reduced by a factor equal exactly to 2, i.e.

$$b_{\text{epi}} = \frac{b_{\text{dia}}}{2}. \quad (9)$$

In practice, however, the above theoretical relation should be verified by a separate calibration process. The same calibration plates as before can be used, but a metallized plate with a step of known height  $h$  is preferable.

### 3.1. The AVAWI( $b$ )–3 technique

The calibration birefringent plate (Fig. 1a and Fig. 3) are used in the same way as before, but is placed on a full mirror to reflect completely light passing through the plate. In twofold passage of light, the birefringent plate behaves as its thickness  $t$  were equal to  $2t$ . Thus, for calibration in reflected light an optimum thickness of the quartz plate (Fig. 1a) is smaller than that for calibration in transmitted light.

If the birefringent prism  $W_2$  No. 2 works, the calibration procedure is exactly the same as for transmitted-light microwinterferometry. On the other hand, the prisms  $W_1$  No. 1 and  $W_1$  No. 3 do not produce in epi-illumination their own interference fringes in the exit pupil of the objective, and interfringe spacings  $b_s$  must be measured in a way described in [6], using a half-shade eyepiece.

### 3.2. The AVAWI( $\lambda$ )–1 technique

A metallized calibration plate with a step of known height  $h$  (Fig.1c) is especially suitable for the calibration procedure in reflected light. When the step is surrounded by an air medium, a highly accurate procedure, referred to as the AVAWI( $\lambda$ )–1 technique can be used (the symbol  $\lambda$  in the round brackets indicates that the object adaptivity functions in the wavelength domain [3]).

The calibration procedure is based on the following equation:

$$\lambda_s = \frac{2h}{m_1 + q_s} = \frac{2h}{m_s} \quad (10)$$

where

$$m_1 = q_s \frac{\lambda_s}{\lambda_1 - \lambda_s}. \quad (11)$$

If the tube birefringent prism  $W_2$ No. 2 works, the calibration procedure is as follows. The calibration step, which has the form of a long stripe, is oriented at right angles to the interference fringes while the objective birefringent prism  $W_0$  is crossed with the tube birefringent prism. Two sheared images of the step are observed and the interference pattern is quite similar to that shown in Fig. 5. The coincident (Fig. 5a) and anticoincident (Fig. 5b) configurations of the undisplaced interference fringes ( $I$ ) and the fringes ( $I'$ ) displaced by the step are sequentially obtained by decreasing

the light wavelength from  $\lambda_1$  to  $\lambda_2, \lambda_3, \dots$ , and the respective interfringe spacings  $b_1, b_2, b_3, \dots$  are measured in the former way (the wedge interference filter WIF is now installed in the epi-illuminator as shown in Figs. 3 and 4 of [5]). Then, the wavelengths  $\lambda_s = \lambda_1, \lambda_2, \lambda_3, \dots$  are calculated from Eq. (10) for a series of the supposed current interference orders  $m_s = m_1 + q_s$ , where  $q_s = 0, 0.5, 1, \dots$ . It is recommended to select such a wavelength for  $\lambda_1$  which is visible as the first one among  $\lambda_s$  in the far red region of the wedge interference filter, knowing that the transmission limit of this filter is at 700 nm.

Finally, the measured interfringe spacings  $b_s = b_1, b_2, b_3, \dots$  are associated with the respective wavelengths  $\lambda_s = \lambda_1, \lambda_2, \lambda_3, \dots$  and the plot  $b(\lambda)$  is made of the paired  $b_s$  and  $\lambda_s$ .

If the tube prism  $W_1$  No. 1 or  $W_1$  No. 3 is calibrated, the principles of the reflected-light uniform-field WAVI method are employed (see [5]). The same Eq. (10) is used for calculating the particular wavelengths  $\lambda_s$ , and the sheared images of the step are adjusted to the maximum darkness of the background of the zero interference order by sliding the wedge interference filter and decreasing the light wavelength from  $\lambda_1$  to  $\lambda_2, \lambda_3, \dots$  (see Fig. 6 in [6] which illustrates very well the situation in question). Since no interference fringes are now observed, the parameters equivalent to the interfringe spacings  $b_s$ , which must be associated with  $\lambda_s$ , are measured with the help of the half-shade eyepiece (see [6]) or by using the balancing method (see [5] and Fig. 5 therein).

## 4. Experiments

To illustrate the calibration procedure in transmitted light based on the AVAWI( $b$ )-3 technique (see Sect. 2.1), a quartz plate of thickness  $t = 653.30 \mu\text{m}$  was used. The result of a calibration process for the tube birefringent prism  $W_2$  No. 2 is Table 4. An exemplary result of the calibration of the tube birefringent prism  $W_2$  No. 2 of a Biolar PI microinterferometer by using a quartz birefringent plate of thickness  $t = 653.30 \mu\text{m}$  and the transmitted-light AVAWI( $b$ )-3 technique

$s$	$q_s$	$b_s [\mu\text{m}]$		$m_s$	$m_s b_s [\mu\text{m}]$		$\bar{b}_s [\mu\text{m}]$	$\lambda [\mu\text{m}]$	$\lambda [\text{nm}]$
		L	R		L	R			
	-1	not observable		8					
1	0	226.65	228.40	9(= $m_1$ )	2039.850	2055.600	227.49	81.6625	730
2	0.5	214.33	216.56	9.5	2036.135	2057.320	215.52	72.5889	655.7
3	1	203.90	205.40	10	2039.000	2054.000	204.74	68.7684	623.4
4	1.5	194.20	195.68	10.5	2039.100	2054.640	194.99	65.3300	594.6
5	2	174.92	187.10	11	2034.120	2058.100	186.13	62.2190	568.6
6	2.5	177.08	179.32	11.5	2036.075	2062.180	178.04	59.3909	545.1
7	3	170.05	171.63	12	2040.600	2059.560	170.62	56.8087	523.8
8	3.5	163.22	164.48	12.5	2040.250	2056.000	163.79	54.4417	504.0
9	4	156.85	157.87	13	2039.050	2052.310	157.49	52.2640	486.0
10	4.5	151.20	152.10	13.5	2041.200	2053.350	151.66	50.2538	469.4
11	5	weakly observable						48.3926	454.1
								46.6643	440.0

shown in Table 4 and Fig. 7. Similar results were obtained for the tube prisms  $W_1$  No. 1 and  $W_1$  No. 3. The data are not given here, since it is only sufficient to multiply the interfringe spacings  $b$  of the plot  $b(\lambda)$  in Fig. 7 by a factor 13.8486 and 4.0502 to obtain the respective plots for the prisms  $W_1$  No. 1 and  $W_2$  No. 3.

On the other hand, to illustrate the calibration procedure also for transmitted light but based on the VAWI-1 technique, a Zeiss refractometric plate was used. The depth  $d$  of its groove was equal to  $12.5425 \mu\text{m} \pm 0.0063 \mu\text{m}$ . The respective results are shown in Table 5 and marked in Fig. 7 by encircled dots.

The same Zeiss plate was also used to demonstrate the calibration of the tube birefringent prism  $W_2$  No. 2 in reflected light. It is self-evident that this plate is equivalent to that with a step (Fig. 1c). It was not metallized, thus the contrast of interference fringes was weak, especially in the blue region of the spectrum. The obtained interfringe spacings  $b_{\text{epi}}$  were equal to  $b_{\text{dia}}/2$  within the measuring accuracy (Table 6).

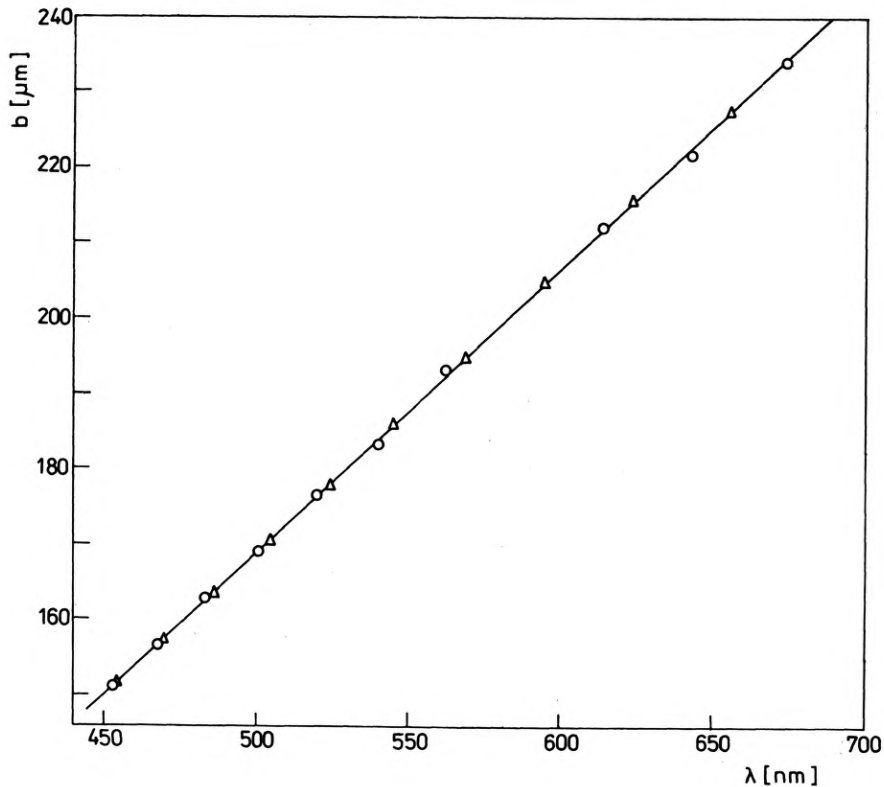


Fig. 7. Calibration plot  $b(\lambda)$  for a Biolar PI microinterferometer used for the work reported here. The plot refers to the tube birefringence prism  $W_2$ . Triangles with dots indicate the calibration points obtained with the quartz plate, while the encircled dots indicate a result of an exemplary calibration process by using the Zeiss microrefractometric plate marked by II in Table 3

Table 5. The ratios  $A_s = \lambda_s / (n_s - 1)$  calculated from Eq. (6) and the wavelengths  $\lambda_s$  read out from the plot  $A(\lambda)$  shown in Fig. 6, for the groove calibration plate II (see Table 3), and the respective interfringe spacings  $b_s$  measured by means of the phase screw (PS, Fig. 2) linked to the transverse movement (p) of the tube birefringent prisms. The data given here refer to the prism W<sub>2</sub>No. 2 operating in dia-illumination. The table illustrates the VAWI-1 technique

$s$	$q_s$	$m_s$	$A_s$ [nm]	$\lambda_s$ [nm]	$b_s$ [ $\mu\text{m}$ ]
	-1	9	1393.61	700	not observable
	-0.5	9.5	1320.26	674.3	234.2
1	0	10(= $m_1$ )	1254.25	642.7	221.7
2	0.5	10.5	1194.52	613.2	211.8
3	1	11	1140.23	586.3	201.7
4	1.5	11.5	1090.65	562.3	193.6
5	2	12	1045.20	540.2	183.3
6	2.5	12.5	1003.40	519.7	176.4
7	3	13	964.81	500.8	169.2
8	3.5	13.5	929.07	483.0	162.8
9	4	14	895.89	467.5	156.4
10	4.5	14.5	865.00	452.7	151.0
11	5	15	836.17	438.5	145.1
12	5.5	15.5	809.19	<430	not observable

Table 6. Wavelengths  $\lambda_s$  calculated from Eq. (10) for the groove depth  $h = 12.5425 \mu\text{m}$ , and respective interfringe spacings  $b_s$  measured by means of the micrometer (phase) screw (PS, Fig. 2) linked to the tube birefringent prisms. The data refer to the prism W<sub>2</sub>No. 2 operating in epi-illumination and light reflected from the groove calibration plate. The table illustrates the AVAWI( $\lambda$ )-1 technique

$s$	$q_s$	$m_s$	$\lambda_s$ [nm]	$b_s$ [ $\mu\text{m}$ ]
	-1	37	677.97	not measurable, low contrast
1	0	38(= $m_1$ )	660.13	114.95
2	1	39	643.21	111.80
3	2	40	627.13	108.63
4	3	41	611.83	105.71
5	4	42	597.26	102.79
6	5	43	583.37	100.23
7	6	44	570.11	98.57
8	7	45	557.44	95.15
9	8	46	545.33	92.85
10	9	47	533.72	90.61
11	10	48	522.60	not measurable, low contrast

## 5. Conclusion

For the calibration in question the most accurate technique is that based on the object-adapted variable wavelength interferometry whose adaptivity functions in the interfringe spacing domain, i.e., the AVAWI( $b$ )-3 technique presented in Sect. 2.1 dealing with transmitted light microinterferometry. The thickness  $t$  of the quartz plate

used was estimated to be determined with a relative error  $\Delta t/t$  not higher than  $\pm 0.01\%$ . Such a well defined thickness makes it possible to achieve a calibration accuracy as follows:  $\Delta\lambda/\lambda = \pm 0.02\%$  and  $\Delta b/b = \pm 0.02\%$ .

The same calibration accuracy is expected in reflected light when a metallized plate with a narrow step or groove is used. In this case the AVAWI( $\lambda$ )-1 technique functions, which is as accurate as the AVAWI( $b$ )-3 technique for transmitted-light double-refracting microinterferometry.

*Acknowledgements* - I wish to thank Mrs H. Nozderko for her help in preparing the drawings.

## References

- [1] PLUTA M., Opt. Appl. 12 (1982), 19-36.
- [2] PLUTA M., Opt. Appl. 15 (1985), 45-51.
- [3] PLUTA M., Opt. Appl. 18 (1988), 75-92.
- [4] PLUTA M., Opt. Appl. 15 (1985), 375-393.
- [5] PLUTA M., Opt. Appl. 16 (1986), 159-174.
- [6] PLUTA M., Opt. Appl. 16 (1986), 141-157.

*Received April 24, 1990*

## Интерферометрия с непрерывно-переменной длиной световой волны. VIII. Калибровка

Определение зависимости между длиной световой волны и межполосным расстоянием является основной калибровочной операцией в интерферометрии. Предложен простой метод калибровки бифракционных микроинтерферометров. Этот метод базируется на адаптивной интерферометрии с переменной длиной световой волны, разработанной в последнее время и представленной в работе из этого цикла. Лишь плитка с двойным лучепреломлением известной толщины или стеклянная с узкой канавкой известной глубины необходимы для выполнения калибровки. Существенной приметой этого метода является то, что калибровка может выполняться в таких же условиях, в каких обычно употребляется микроинтерферометр.